9th AUSTRALASIAN
FLUID MECHANICS CONFERENCE,
AUCKLAND, 8-12 DECEMBER 1986

Flow in Grooved Channels

J. J. J. CHEN[1], Y. C. LEUNG[2] and N. W. M. KO[2]

[1]Department of Chemical & Materials Engineering, University of Auckland, New Zealand.
[2]Mechanical Engineering Department, University of Hong Kong, Hong Kong.

ABSTRACT

Experimental results for the frictional pressure drop in a square channel with longitudinal grooves are presented. It is found that the frictional pressure drop behaviour is dependent on the characteristic dimensions of these grooves. In the turbulent flow region, the pressure drops are greater than those for an equivalent smooth channel and may be predicted using the "Law of the wall". In some cases, it is observed that there is a delay in the transition from laminar to turbulent flow such that in the range where turbulent flow is normally expected, a reduction in drag is observed.

INTRODUCTION

Finned tubes have been used to augment heat transfer in heat exchangers. This augmentation is often attributed to the increase in surface area, and the ability of these fins in promoting liquid entrainment and increasing interfacial shear (Webb 1981, Royal and Bergles 1976).

Drag measurements have also been carried out for flow in triangular channels with acute angles and external flow over grooved surfaces, see, e.g. Carlson and Irvine (1961), Walsh (1980), Walsh and Weinstein (1979). Under certain conditions, it had been found that a reduction in drag may result. As decreased heat transfer is generally associated with reduced drags, it would be beneficial to determine if, in fact, reduced drag takes place in grooved channels, and the conditions under which this occurs. In addition, this phenomena of passive drag reduction may also be used to advantage.

Subsequently, Chen et al (1986) determined the conditions under which drag reduction would take place in the internal flow of water and air in a grooved channel (Chen et al 1983).

EXPERIMENTAL EQUIPMENT

The experimental equipment has also been presented elsewhere (Chen et al 1986, Leung 1986). A schematic diagram is shown in Figure 1 and it consists of a closed circuit water loop. Town water was used in the tests and was changed after each series of tests. A constant head tank at a height of 3m above floor level supplied water through a control valve into the horizontal test section preceded by a 0.7m long calming section which was found to be adequate for the development of the pressure profile. After the test section, the water discharged into a calibrated measurement tank which was connected to a reservoir. The reservoir supplied water via a pump to the constant head tank. By-pass was provided on the high pressure side of the pump so as to regulate the amount of water being pumped up to the constant head tank. To ensure that the head was constant there must be an overflow of water from the constant head tank into the reservoir. A valve was provided between the measurement tank and the reservoir to facilitate the measurement of flow rate using a stop watch.

The test section may be easily removed and substituted by any one of the eleven channels fabricated for testing. Each time this was carried out, care was exercised to ensure alignment. The channels were fabricated with the characteristic dimensions as listed in Table 1. The process of manufacture involved first milling longitudinal grooves on to 4 pieces of 6mm thick flat PVC sheets of nominal dimensions 700mm x 30mm. After machining, the sheets were cut to size and assembled by gluing at the corners to form the square test channels. The size of the grooves and the length of the test section were therefore dictated by the size of the cutting tool and the length of the stroke of the milling machine respectively.

Pressure tapping points were provided at the side and at the top of the test section at a distance of 0.4m apart and U-tube manometers using carbon tetrachloride (S.G. 1.59) was used as the manometer fluid. The readings obtained from the side tappings were identical to those from the tappings at the top. Experiments were performed with the water flow rate ranging between 100 to 1700 $cm^3\ s^{-1}$ corresponding to a Reynolds number range of 4×10^3 to 7×10^4 based on the hydraulic diameter of the ungrooved channel.

EXPERIMENTAL RESULTS

A complete set of experimental results is given in Leung (1986) and Chen et al (1986). Friction factor and Reynolds number defined as follows has been used and its rationale has been given in Chen et al (1986) for the conditions under consideration

$$f = \left(\frac{dP}{dL}\right) \frac{D}{\frac{1}{2}\rho u^2} \qquad (1)$$

$$Re = \frac{\rho u D}{\mu} \qquad (2)$$

where D is the hydraulic diameter based on the square section formed by the mean heights of the grooves.

Consequently, data are presented as f vs Re in Figures (2) and (3) for channels number 3 and 6 which are typical of the data obtained. Also shown in the figures is the Prandtl equation applicable for a smooth pipe flow situation.

$$\frac{1}{\sqrt{f}} = 2.035 \log Re\sqrt{f} - 0.8 \qquad (3)$$

The results for the ungrooved channel, i.e. number 1, when plotted as friction factor versus Reynolds number using the hydraulic diameter concept, are

slightly above the line for smooth circular pipe indicating that the surfaces are not hydraulically smooth. This is acceptable as Schlichting (1979) had found that the hydraulic diameter concept represents data for smooth-walled square-sectioned flow channels. In fact, the results may be represented using the Colebrook-White equation (1939) with a roughness ratio of 0.0004.

The general trend is that the experimental results begin to increase with Re to above that given by the Prandtl equation. The data appear to indicate that it is part of a late or delayed transition, but as Re is increased further the data then approach lines which are somewhat parallel, but higher than that given by equation (3), depending on the characteristics of the grooves.

The conditions under which the value of f increase and cross-over the smooth-pipe line have already been given in Chen et al (1986), i.e. the conditions under which drag reduction may occur. These conditions are in agreement with those given by Walsh (1980), i.e. when $h^+<25$ and $S^+<100$ where h^+ and S^+ are the height and spacing of grooves expressed in terms of the "Law of the Wall" co-ordinates. In addition, the effects of apex angle and groove depth on the cross-over have also been examined by Chen et al (1986).

A SIMPLE ANALYSIS

The detailed analysis is given in Leung (1986). It follows closely that given by Scott and Webb (1981) making use of the "Law-of-the-Wall" (Schlichting 1979) which, for the turbulent-dominated wall region ($y^+>26$), is given by

$$\frac{u}{u*} = 2.5 \ln\left(\frac{yu*}{\nu}\right) + 5.5 \qquad (4)$$

By considering the grooved region and the core region separately, and the reduced core velocity due to the presence of the grooves, it is possible to show that, for grooved channels,

$$\sqrt{(8/f)} = (2.5 \ln \tfrac{1}{2} Re \sqrt{(f/8)} + 1.75) - K \qquad (5)$$

where

$$K = 2.5 \ln\frac{D}{2h\sin\alpha} + 2.5 \frac{Ac}{A_T}\frac{\ell^2}{(\ell-h)^2}\left(1 + \ln\frac{h}{\ell} - \frac{h}{\ell}\right)$$

It is noted that equation (5) is similar to that for a smooth channel except that the entire expression is shifted by a factor thus resulting in a higher value of f for the grooved channel. Equation (5) may be written in the general form

$$\frac{1}{\sqrt{f}} = 2.035 \log Re \sqrt{f} - B \qquad (6)$$

when B is tabulated in Table 2 for the various channels dealt with in this work. When B=0.8, equation (6) reduces to equation (3), the Prandtl equation.

DISCUSSIONS

In a previous paper (Chen et al 1986), we have discussed the conditions where drag reduction occurs in terms of h^+ and S^+ the height and spacing expressed in terms of the "Law-of-the-Wall" co-ordinates, the apex angle, and the physical height of the grooves.

With the presence of grooves, the flow undergoes a gradual and extended transition from laminar to turbulent flow at a value of Reynolds number higher than is normally associated with closed conduit flows. While it isnot known how exactly this delay in transition is effected, conditions when this occurs may be predicted using the h^+ and S^+ values, namely, at $h^+<25$ and $S^+<100$. No data were available for flows with Reynolds number below 5×10^3 as the apparatus employed was not suitable for work in the low Reynolds number range.

Beyond the point where the value of the friction factor reaches a maximum and begins to settle down indicating fully turbulent flow, the data approach the predictions given by equation (6) as shown in Figures 2 and 3.

CONCLUSIONS

It has been shown that there is a delay in the laminar to turbulent transition in the flow of water in a grooved channel. Although it is not known exactly how this delay mechanism works, it is possible to predict the range of conditions when this occurs. This delay in transition results in a reduction in drag where normally turbulent flow is expected to have occurred. In the range of conditions studied, the transition to turbulent flow occurs at a much higher Reynolds number, approximately an order of magnitude higher than that normally expected.

After transition to turbulent flow, the friction factor exhibits an increase compared to those for a smooth pipe. In this region, the increased friction factors may be predicted using the "Law-of-the-Wall".

NOMENCLATURE

- A_c Channel flow area excluding the grooved regions.
- A_T Total channel flow area.
- B A factor in equation (6).
- D Hydraulic diameter based on mean groove height.
- f Friction factor.
- h Groove height.
- h^+ Groove height in terms of the "Law-of-the-Wall" coordinates, $= (hu/\nu)(f/8)^{1/2}$.
- K A factor in equation (5).
- L Longitudinal distance.
- ℓ Half nominal width of channel.
- P Pressure.
- Re Reynolds number.
- S Groove width.
- S^+ Groove width in terms of the "Law-of-the-Wall" coordinates $= (Su/\nu)(f/8)^{1/2}$
- u Axial velocity.
- u* Friction velocity, $= (\tau/\rho)^{1/2}$.
- y Perpendicular distance from wall.

Greek Symbols

- α Groove apex angle.
- μ Fluid viscosity.
- ν Fluid kinematic viscosity.
- ρ Fluid density.
- τ Shear at wall.

REFERENCES

Carlson, L.W.; Irvine,T.F.(1961): Fully developed pressure drop in triangular shaped ducts, J.Heat Transfer, 83, 441-444.

Chen, J.J.J.; Leung, Y.C.; Ko, N.W.M.(1986): Drag reduction in a longitudinally-grooved channel, Ind.Eng.Chem.,Fundam., (To appear).

Chen, J.J.J.; Ho,C.M.; Chan, Y.M.(1983): Unpublished work, c.f., Ho.C.M., B.Sc. Dissertation (1983) and Chan, Y.M., B.Sc. Dissertation (1983), University of Hong Kong.

Colebrook, C.F.(1939): Turbulent flow in pipes, with particular reference to the transition region between smooth and rough pipe laws, J. Instn.Civ. Engrs., 11, 133-156.

Leung, Y.C.(1986): Ph.D. Thesis (In preparation), University of Hong Kong.

Royal, J.H.; Bergles, A.E.(1978): Augmentation of horizontal in tube condensation by means of twisted-taped inserts and internally finned tubes, J.Heat Transfer, 100, 17-24.

Schlichting, H.(1979) Boundary Layer Theory, 7th Ed., McGraw-Hill Book Co, New York.

Scott, M.J.; Webb, R.L.(1981): Analytic prediction of the friction factor for turbulent flow in internally finned channels, J.Heat Transfer, 103, 423-428.

Walsh, M.J.(1980), Drag characteristics of V-groove and transverse curvature riblets, in Viscous Flow Drag Reduction, G.R.Hough (Ed), pp168-184, AIAA.

Walsh, M.J.; Weinstein, L.M.(1979): Drag and heat-transfer characteristics of smalllongitudinally ribbed surfaces, AIAA J., 17, 770-771.

Webb, R.L.(1981): Performance evaluation criteria for use of enhanced heat transfer surfaces in heat exchanger design, Int. J. Heat Mass Transfer, 24, 715-726.

Figure 1. Schematic diagram of the experimental apparatus.

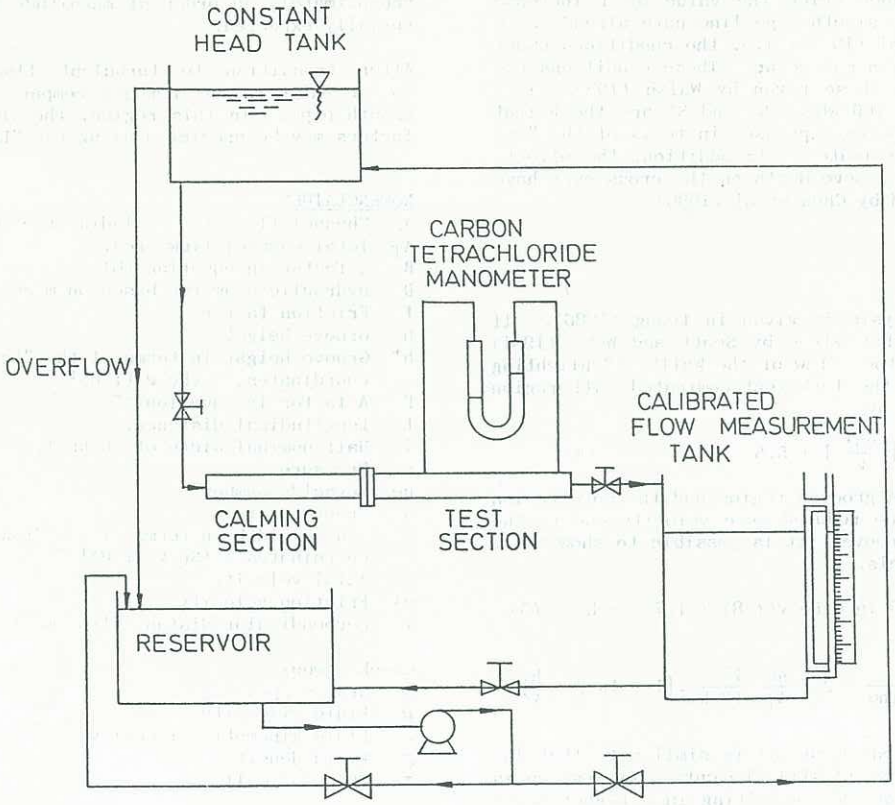

Figure 2. Experimental data for channel no.3 plotted as f vs Re. The solid line represents equation (3), and the broken line represents equation (6) with B obtained from Table 2.

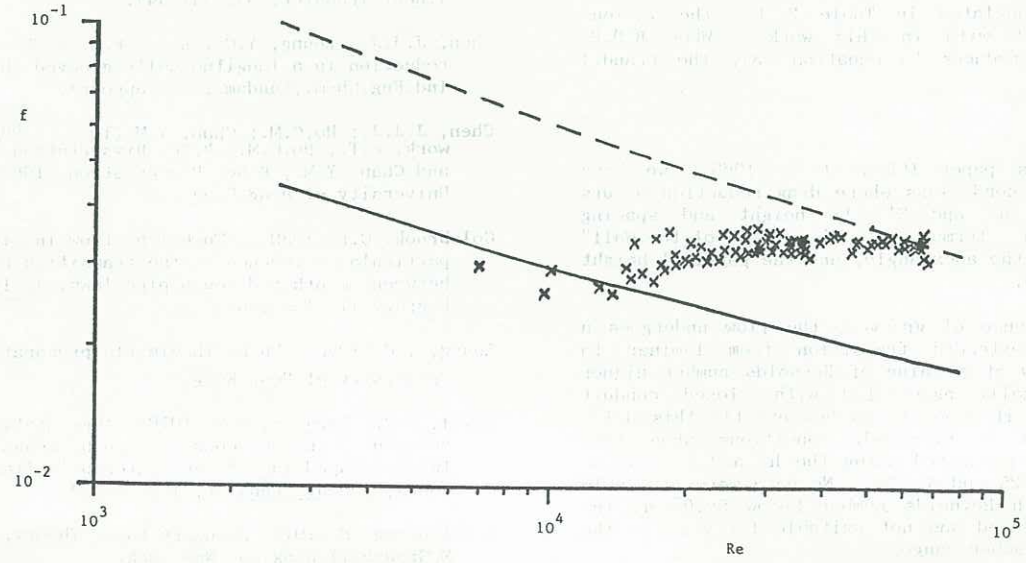

Figure 3. Experimental data for channel no.6 plotted as f vs Re. The solid line represents equation (3), and the broken line represents equation (6) with B obtained from Table 2.

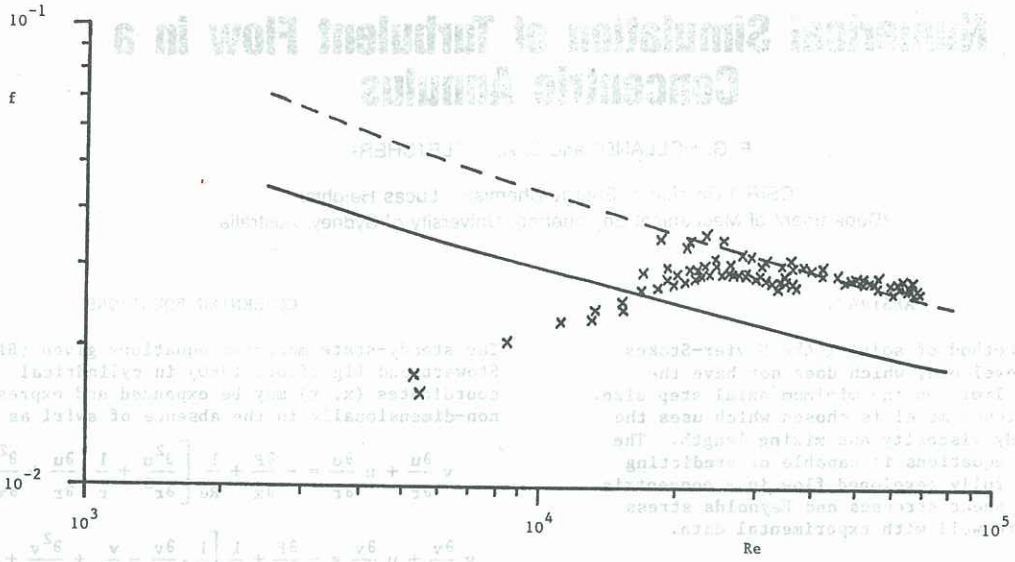

Table 1a. Dimensions of channels used in the experiments

Model No.	1	2	3	4	5	6	7	8	9	10	11
Groove height h mm	–	0.29	0.50	0.50	0.50	0.50	0.70	0.70	1.00	0.50	0.50
Groove spacing s mm	–	0.61	0.35	0.43	0.65	1.04	0.63	1.45	2.06	2.08	2.08
Groove width mm	–	–	–	–	–	–	–	–	–	–	1.00
Groove apex angle	–	90°	30°	45°	60°	90°	45°	90°	90°	90°	–
Actual wetted perimeter (mm)	100.0	134.5	295.8	251.7	177.6	136.0	240.5	136.5	137.3	119.9	148.0
D_M (mm)	25.00	25.29	25.50	25.50	25.50	25.50	25.70	25.70	26.00	25.24	25.48
D_H (mm)	25.00	19.02	8.79	10.33	14.64	19.13	10.98	19.35	19.69	21.25	17.54

Table 1b. Profiles of Grooves in Channel Walls

Model No.	Description
2, 3, 4, 5, 6, 7, 8, 9	
10	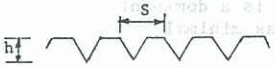
11	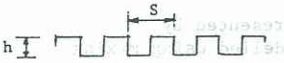

Table 2 Values of B in Equation (6).

Channel No.	2	3	4	5	6	7	8	9	10	11
Value of B.	2.02	2.86	2.53	2.28	1.97	2.48	1.94	1.88	2.07	2.11